



THE UNIVERSITY *of* EDINBURGH

Edinburgh Research Explorer

Combined Lattice and Continuum Analysis of the Light Quark $V-A$ Correlator at NNLO in ChPT

Citation for published version:

A. Boyle, P. Del Debbio, L. Garron, N. J. Hudspith, R. Kerrane, E. Maltman, K & M. Zanotti, J 2013, 'Combined Lattice and Continuum Analysis of the Light Quark $V-A$ Correlator at NNLO in ChPT', *Proceedings of Science*, vol. 2013, no. LATTICE 2013, 306.

Link:

[Link to publication record in Edinburgh Research Explorer](#)

Published In:

Proceedings of Science

General rights

Copyright for the publications made accessible via the Edinburgh Research Explorer is retained by the author(s) and / or other copyright owners and it is a condition of accessing these publications that users recognise and abide by the legal requirements associated with these rights.

Take down policy

The University of Edinburgh has made every reasonable effort to ensure that Edinburgh Research Explorer content complies with UK legislation. If you believe that the public display of this file breaches copyright please contact openaccess@ed.ac.uk providing details, and we will remove access to the work immediately and investigate your claim.



L_{10}^r From a Combined NNLO Lattice, Continuum Analysis of the Light Quark $V - A$ Correlator

**P.A. Boyle,^a L. Del Debbio,^a N. Garron,^b R.J. Hudspith,^a E. Kerrane^c, K. Maltman^{*},
^{d,e} and J.M. Zanotti^e**

^a*Physics and Astronomy, University of Edinburgh, Edinburgh EH9 3JZ, UK*

^b*School of Mathematics, Trinity College, Dublin 2, Ireland*

^c*Instituto de Física Teórica UAM/CSIC, Universidad Autónoma de Madrid, Cantoblanco
E-28049 Madrid, Spain*

^d*Mathematics and Statistics, York University, Toronto M3J 1P3 Canada*

^e*CSSM, University of Adelaide, Adelaide 5005 Australia*

*E-mail: paboyle@ph.ed.ac.uk, ldeldebb@ph.ed.ac.uk,
ngarron@maths.tcd.ie, s0968574@sms.ed.ac.uk,
eoin.kerrane@gmail.com, kmaltman@yorku.ca,
james.zanotti@adelaide.edu.au*

A combination of lattice and continuum data for the light-quark V-A correlator, supplemented by results from a chiral sum-rule analysis of the flavor-breaking flavor $ud-us$ V-A correlator difference, is shown to make possible a high-precision NNLO determination of the renormalized NLO chiral low-energy constant L_{10}^r . Key to this determination is the ability to simultaneously fix the two combinations of NNLO low-energy constants also entering the analysis. With current versions of the strange hadronic τ branching fractions required as input to the flavor-breaking V-A sum rule, we find $L_{10}^r(m_\rho) = -0.00346(29)$. This represents both the best current precision for L_{10}^r , and the first NNLO determination having all errors under full control.

*31st International Symposium on Lattice Field Theory LATTICE 2013
July 29 - August 3, 2013
Mainz, Germany*

^{*}Speaker.

1. Introduction

The low-energy effective (chiral) Lagrangian framework encodes, in the most general way, the constraints on the light degrees of freedom of the symmetries and approximate chiral symmetry of QCD. A key goal in maximizing the predictive power of this approach is the completion and/or improvement of the determinations of all coefficients (low-energy constants, or LECs) accompanying operators allowed by the symmetry arguments out to a given order in the chiral expansion. In this paper we focus on an improved, next-to-next-to-leading order (NNLO) determination of the renormalized next-to-leading order (NLO) LEC L'_{10} . The analysis also yields values for two NNLO LEC combinations, the determination of which is crucial to reducing the uncertainty on L'_{10} .

Existing determinations of L'_{10} are based on analyses of the low- Q^2 behavior of the difference, $\Delta\Pi_{V-A}(Q^2) \equiv \Pi_{ud;V-A}^{(0+1)}(Q^2)$, of the light-quark (flavor ud) vector (V) and axial vector (A) correlators. The spin $J = 0, 1$ scalar correlators $\Pi_{ud;V/A}^{(J)}(Q^2)$ entering this definition are defined by the standard decompositions of the ud V and A current-current two-point functions. An NLO version of this analysis was performed in Ref. [1], with differential hadronic τ decay distribution results for the spectral function, $\Delta\rho_{V-A}(s)$, of $\Delta\Pi_{V-A}(Q^2)$ used to fix $\Delta\Pi_{V-A}(0)$, and hence L'_{10} , the only free parameter in the NLO representation of $\Delta\Pi_{V-A}(0)$. NLO analyses were also performed using low-(Euclidean)- Q^2 lattice data for $\Delta\Pi_{V-A}(Q^2)$ [2, 3].

The low-energy representations of $\Pi_{ud;V/A}^{(J)}(Q^2)$ are now known to NNLO [5], and yield a value for the coefficient of L'_{10} in the resulting $\Delta\Pi_{V-A}(0)$ representation $\sim 50\%$ larger at NNLO than at NLO, raising doubts about the reliability of the earlier NLO analyses. The observation (also made for the ud V correlator [4]) that the NLO representation fails completely to reproduce the variation of $\Delta\Pi_{V-A}(Q^2)$ with Q^2 [7] confirms these worries. Attempts to extend the continuum NLO analysis to NNLO, however, run into the problem that the NNLO representation of $\Delta\Pi_{V-A}(0)$ involves two additional NNLO LEC combinations, one of which is completely unknown. In Ref. [6], this combination was assigned a central value zero, and a rough guess at the error (based only on large- N_c counting, and since argued to be rather non-conservative [7]) attributed to this choice. This error turns out to completely dominate the uncertainty on the resulting determination of L'_{10} [6].

In this paper, we address this situation, showing how to combine the dispersive determination of $\Delta\Pi_{V-A}(0)$ with lattice data and an additional flavor-breaking (FB) chiral sum rule to fix simultaneously L'_{10} and the two NNLO LEC combinations noted above. Section 2 provides more detail on the dispersive determination of $\Delta\Pi_{V-A}(0)$, the NNLO representation of $\Delta\Pi_{V-A}(Q^2)$, and the problems encountered in an NNLO continuum analysis. The use of lattice data and a new chiral sum rule, involving L'_{10} and one of the two NNLO LEC combinations, to deal with these problems is then also discussed. Section 3 presents the results of our analysis.

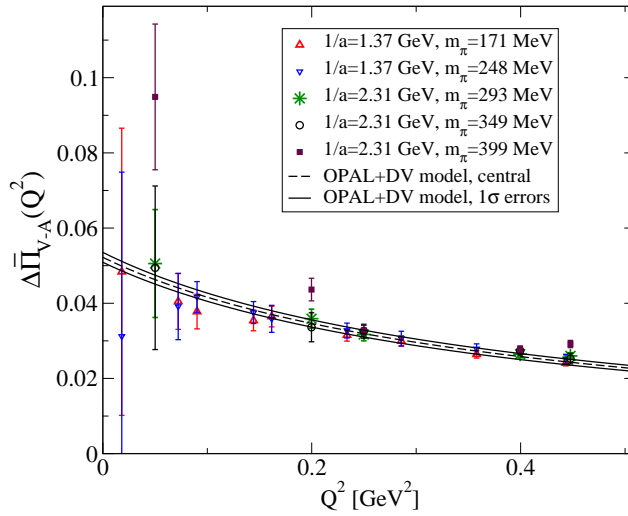
2. Ingredients for the NNLO Determination of L'_{10}

$\Delta\Pi_{V-A}(Q^2)$ is free of kinematic singularities and satisfies an unsubtracted dispersion relation. With $\Delta\bar{\Pi}_{V-A}(Q^2)$ and $\Delta\bar{\rho}_{V-A}(s)$ the continuum (π -pole-subtracted) versions of $\Delta\Pi_{V-A}(Q^2)$ and $\Delta\rho_{V-A}(Q^2)$, the dispersion relation, written here for spacelike $Q^2 = -q^2 = -s$, becomes

$$\Delta\bar{\Pi}_{V-A}(Q^2) = \int_{4m_\pi^2}^{\infty} ds \frac{\Delta\bar{\rho}_{V-A}(s)}{s + Q^2}. \quad (2.1)$$

This representation was recently used to generate high-precision results for $\Delta\overline{\Pi}_{V-A}(Q^2)$ [7]. The spectral functions, $\Delta\overline{\rho}_{V/A}(s)$, needed on the RHS, are accessible up to $s = m_\tau^2$ using OPAL hadronic τ decay data [8]. These have been updated for current branching fractions [9]. Above $s = m_\tau^2$, the representation of $\Delta\overline{\rho}_{V/A}(s)$ as a sum of 5-loop $D = 0$ OPE and duality violating contributions, studied in great detail in Refs. [9], was employed. For low Q^2 , the part of the integral involving the experimental spectral data strongly dominates the results for $\Delta\overline{\Pi}_{V-A}(Q^2)$ [7].

Figure 1: Continuum and RBC/UKQCD lattice results for $\Delta\overline{\Pi}_{V-A}(Q^2)$ in the low- Q^2 region



For $Q^2 > 0$, $\Delta\overline{\Pi}_{V-A}(Q^2)$ can also be determined on the lattice for a range of $m_u = m_d$ and m_s . Ensemble m_π and f_π values then yield the corresponding $\Delta\overline{\Pi}_{V-A}(Q^2)$. We work here with results for five RBC/UKQCD $n_f = 2 + 1$, domain wall fermion ensembles: three, with $m_\pi = 293, 349$ and 399 MeV, having inverse lattice spacing $1/a = 2.31$ GeV, and two, with $m_\pi = 171, 248$ MeV, having $1/a = 1.37$ GeV. Full simulation details may be found in Refs. [10, 11].

Lattice and continuum results for $\Delta\overline{\Pi}_{V-A}(Q^2)$ are shown, for $Q^2 < 0.5$ GeV², in Fig. 1. The continuum and near-physical-mass, $m_\pi = 171$ MeV, lattice results are in very good agreement. This agreement persists to much higher Q^2 than shown here, suggesting lattice artefacts are safely under control. Lattice errors are larger than continuum ones below $Q^2 \sim 0.3$ GeV², particularly so for Q^2 near 0, where, for Euclidean Q , the kinematic factors multiplying the scalar correlators in the spin decomposition of the two-point functions (hence also the two-point functions themselves) vanish in the limit $Q^2 \rightarrow 0$.

The NNLO representation of $\Delta\overline{\Pi}_{V-A}(Q^2)$ has the form [5]

$$\Delta\overline{\Pi}_{V-A}(Q^2) = c_{10} L_{10}^r + \mathcal{C}_0^r + \mathcal{C}_1^r + c_9 L_9^r + R(Q^2) - 16C_{87}^r Q^2, \quad (2.2)$$

where all quantities other than Q^2 on the RHS depend on the chiral renormalization scale, μ , and

$$c_9 = 16(2\mu_\pi + \mu_K), \quad c_{10} = -8(1 - 8\mu_\pi - 4\mu_K) \quad (2.3)$$

$$\mathcal{C}_0^r \equiv 32m_\pi^2 (C_{12}^r - C_{61}^r + C_{80}^r), \quad \mathcal{C}_1^r \equiv 32 (m_\pi^2 + 2m_K^2) (C_{13}^r - C_{62}^r + C_{81}^r), \quad (2.4)$$

with $\mu_P = \frac{m_P^2}{32\pi^2 f_\pi^2} \log\left(\frac{m_P^2}{\mu^2}\right)$, and C_k^r the dimensionful renormalized NNLO LECs of Ref. [12]. \mathcal{C}_0^r and \mathcal{C}_1^r are leading order in N_c and $1/N_c$ suppressed, respectively. The rather lengthy expression for $R(Q^2)$ is omitted but easily reconstructed from the results of Sections 4, 6 and Appendix B of Ref. [5]. For given Q^2 , $R(Q^2)$ depends only on μ , f_π and the pseudoscalar (PS) meson masses [5]. In what follows, we define $\hat{R}(Q^2) \equiv c_9 L_9^r + R(Q^2)$, employ $L_9^r(0.77 \text{ GeV}) = 0.00593(43)$ [17], and treat $\hat{R}(Q^2)$ as known once Q^2 , μ , f_π and the PS masses are fixed.

Eq. (2.2) makes evident the problem encountered in attempting to extend the NLO L_{10}^r determination to NNLO. At NLO, with $[R(0)]_{NLO}$ exactly known, the result $\Delta\bar{\Pi}_{V-A}(0) = 0.0516(7)$ [7] translates into a nominally very precise value for L_{10}^r . At NNLO, however, the constraint becomes

$$\Delta\bar{\Pi}_{V-A}(0) = 0.0516(7) = c_{10} L_{10}^r + \mathcal{C}_0^r + \mathcal{C}_1^r + \hat{R}(0), \quad (2.5)$$

and input for $\mathcal{C}_{0,1}^r$ is required to turn this into a determination of L_{10}^r . Ref. [6] dealt with this problem using existing determinations of C_{12}^r [13] and C_{61}^r [14, 15], a resonance ChPT (RChPT) estimate for C_{80}^r [16], and a large- N_c -motivated guess for \mathcal{C}_1^r . The ~ 26 enhancement of the mass-dependent factor in \mathcal{C}_1^r relative to that in \mathcal{C}_0^r more than compensates for the $1/N_c$ LEC suppression, making the lack of a physically constrained estimate for \mathcal{C}_1^r particularly problematic.

A key point in resolving this problem is the observation that c_{10} , \mathcal{C}_0^r and \mathcal{C}_1^r depend differently on $m_{\pi,K}$. Lattice data with variable m_q can thus help disentangle the different contributions. Considering the difference of the physical ('*phys*') and lattice ('*latt*') versions of $\Delta\bar{\Pi}_{V-A}(Q^2)$ at the same Q^2 , and implementing the NNLO representation for both, yields the new constraints

$$[\Delta\bar{\Pi}_{V-A}(Q^2)]_{latt} - [\Delta\bar{\Pi}_{V-A}(Q^2)]_{phys} - \Delta\hat{R}(Q^2) = \Delta c_{10}^r L_{10}^r + \Delta c_0^r \mathcal{C}_0^r + \Delta c_1^r \mathcal{C}_1^r, \quad (2.6)$$

where $\Delta\hat{R}(Q^2) \equiv [\hat{R}(Q^2)]_{latt} - [\hat{R}(Q^2)]_{phys}$, and the expressions for Δc_{10} , Δc_0 , Δc_1 follow from those for c_{10} , c_0 and c_1 . Δc_{10} , Δc_0 and Δc_1 are all fixed by μ and the physical and ensemble PS mass and f_π values; $\Delta\hat{R}(Q^2)$ depends, in addition, on Q^2 . For all ensembles considered here, the combination of L_{10}^r , \mathcal{C}_0^r and \mathcal{C}_1^r in (2.6) differs significantly from that in (2.5). Since the RHS of Eq. (2.6) is Q^2 -independent, while all terms on the LHS are Q^2 -dependent, the constraints (2.6), for a given ensemble, but different Q^2 , provide checks on the self-consistency of the analysis.

The combination of the lattice constraints (2.6) and continuum constraint (2.5) is sufficient to allow a simultaneous determination of L_{10}^r , \mathcal{C}_0^r and \mathcal{C}_1^r , albeit with larger-than-ideal errors ($\sim 25\%$, $\sim 100\%$ and $\sim 80\%$, respectively), which result from the sizable uncertainties on the low- Q^2 lattice data. An additional constraint is required to reduce these errors.

Such a constraint can be obtained from inverse moment finite energy sum rules (IMFESRs) involving the FB $ud - us$ V-A correlator difference, $\Delta\Pi_{V-A}^{FB} \equiv \Pi_{ud;V-A}^{(0+1)} - \Pi_{us;V-A}^{(0+1)}$ [18]. Generically, for polynomial $w(s)$, these have the form

$$w(0)\Delta\Pi_{V-A}^{FB}(0) = \frac{1}{2\pi i} \oint_{|s|=s_0} ds \frac{w(s)}{s} \Delta\Pi_{V-A}^{FB}(Q^2) + \int_0^{s_0} ds \frac{w(s)}{s} \Delta\rho_{V-A}^{FB}(s). \quad (2.7)$$

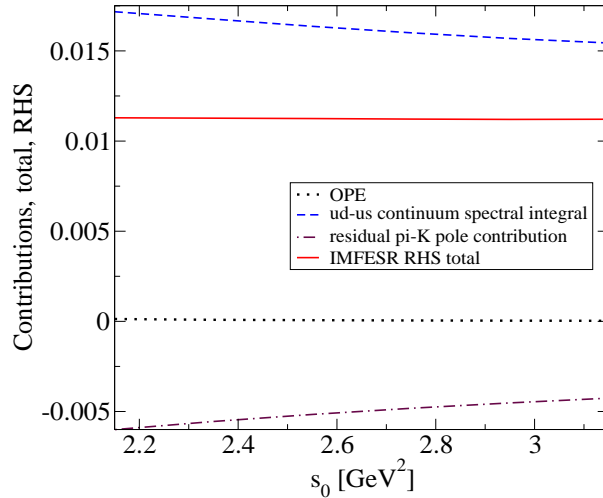
The first term on the RHS is to be evaluated using the OPE, the second using experimental spectral data. The result is a constraint on the LECs appearing in the low-energy representation of the

LHS. The choice $w(s) = w_{DK}(y) = (1-y)^3(1+y+\frac{1}{2}y^2)$ with $y = s/s_0$, reduces OPE errors and strongly suppresses spectral contributions from the high- s region where uncertainties in the us V/A separation are large [14]. With $\Delta\bar{\Pi}_{V-A}^{FB}$ ($\Delta\bar{\rho}_{V-A}^{FB}$) the π - and K -pole subtracted version of $\Delta\Pi_{V-A}^{FB}$ ($\Delta\rho_{V-A}^{FB}$), $y_\pi = m_\pi^2/s_0$, $y_K = m_K^2/s_0$, and $f_{res}(y) = 4y - y^2 - y^3 - y^4 + y^5$, (2.7) can be recast as

$$\begin{aligned} \Delta\bar{\Pi}_{V-A}^{FB}(0) &= \frac{1}{2\pi i} \oint_{|s|=s_0} ds \frac{w_{DK}(y)}{s} [\Delta\Pi_{V-A}^{FB}(Q^2)]^{OPE} \int_{4m_\pi^2}^{s_0} ds \frac{w_{DK}(y)}{s} \Delta\bar{\rho}_{V-A}^{FB}(s) \\ &\quad + \frac{f_\pi^2}{m_\pi^2} f_{res}(y_\pi) - \frac{f_K^2}{m_K^2} f_{res}(y_K). \end{aligned} \quad (2.8)$$

The s_0 -independence of the LHS provides a self-consistency test for the treatments of the individual s_0 -dependent terms appearing on the RHS. This test is well satisfied, as shown in Fig. 2 [18]. Strong cancellations, already present in the separate ud and us $D = 2, 4$ V-A series, make the OPE contributions very small. Updated [9] OPAL data [8] were employed for the ud spectral integrals. For the us spectral integrals, recent B-factory results were used for $K\pi$ [20], $K^-\pi^+\pi^-$ [21], and $K_S\pi^-\pi^0$ [22], and ALEPH data [23], rescaled to current branching fractions, for all other modes. The us V/A separation is unambiguous for K (A) and $K\pi$ (V) contributions, as well as for $K^-\pi^+\pi^-$ and $K_S\pi^-\pi^0$ contributions in the $K_1(1270)$ (A) region. The $1/s$ and $w_{DK}(y)$ weightings (the latter with its triple zero at $s = s_0$) mean these contributions dominate the us spectral integrals. Higher- s $K\pi\pi$ contributions, and those from all higher multiplicity modes, are assigned $50 \pm 50\%$ each to the V and A channels, with full anticorrelation.

Figure 2: s_0 -dependence of the individual contributions and sum on the RHS of the FB V-A IMFESR.



The use of the combination $\Delta\bar{\Pi}_{V-A}^{FB}$ is predicated on the fact that the NNLO representation

$$\left[\Delta\bar{\Pi}_{V-A}^{FB}(0) \right]_{NNLO} = R_{V-A}^{FB}(0) + c'_5 L_5^r + c'_9 L_9^r + c'_{10} L_{10}^r - 32 \left(\frac{m_K^2 - m_\pi^2}{m_\pi^2} \right) \mathcal{C}_0^r \quad (2.9)$$

involves a combination of L_{10}^r and \mathcal{C}_0^r independent of those appearing in (2.5) and (2.6). $R_{V-A}^{FB}(0)$, c'_5 , c'_9 and c'_{10} are, as usual, determined by μ , f_π and the PS masses. Evaluating all LECs at the conventional chiral scale choice, $\mu = \hat{\mu} = 0.77 \text{ GeV}$, the results of Ref. [5] imply

$$\left[\Delta \bar{\Pi}_{V-A}^{FB}(0) \right]_{NNLO} = 0.00670 - 0.722L_5^r + 1.423L_9^r + 2.125L_{10}^r - 11.606\mathcal{C}_0^r, \quad (2.10)$$

which, with $L_5^r(\hat{\mu}) = 0.00058(13)$ [19] and $L_9^r(\hat{\mu}) = 0.00593(43)$ [17], yields the new constraint

$$2.125L_{10}^r - 11.606\mathcal{C}_0^r, = \Delta \bar{\Pi}_{V-A}^{FB}(0) - 0.01472(61)_{L_9^r} (9)_{L_5^r}. \quad (2.11)$$

3. Results

The results of the continuum $\Delta \bar{\Pi}_{V-A}(Q^2)$ study of Ref. [7] make clear that the combined lattice/continuum constraints can be safely employed only for Q^2 up to $\sim 0.3 \text{ GeV}^2$. For the fine ensembles, this leaves only a few Q^2 points with errors small enough to allow for meaningful self-consistency tests. One of the constraints for the $m_\pi = 399 \text{ MeV}$ fine ensemble appears clearly out of line, but given the limited number of points, we exclude the constraints from this ensemble, and base our fits on results from the other four ensembles, which display mutually consistent constraints for all relevant Q^2 . The results are, in fact, essentially unchanged if the lack of self-consistency for the fifth ensemble is ignored, and all ensembles included in the fit.

Results of the 1st-stage fit, to the $\Delta \Pi_{V-A}(0)$ and combined lattice-continuum constraints, are

$$L_{10}^r(\hat{\mu}) = -0.0031(8), \quad \mathcal{C}_0^r(\hat{\mu}) = -0.00081(82), \quad \mathcal{C}_1^r(\hat{\mu}) = 0.014(11). \quad (3.1)$$

The non-trivial uncertainties result from the need to determine two additional LEC combinations from the relatively large-error lattice data. Strong correlations among the fit parameters mean the additional IMFESR constraint has the possibility of improving all three errors.

The input outlined above yields the following result for the RHS of Eq. (2.8):

$$\Delta \bar{\Pi}_{V-A}^{FB}(0) = 0.01125(135)_{OPAL} (16)_{res} (15)_{OPE} (5)_{s_0}. \quad (3.2)$$

The subscripts '*OPAL*', '*res*', '*OPE*' and '*s₀*' label errors associated with uncertainties in the OPAL continuum distributions, residual π - and K -pole and OPE contributions, and the (very small) residual s_0 -dependence, respectively. Adding the resulting IMFESR constraint to the combined fit yields

$$L_{10}^r(\hat{\mu}) = -0.00346(29), \quad \mathcal{C}_0^r(\hat{\mu}) = -0.00034(12), \quad \mathcal{C}_1^r(\hat{\mu}) = 0.0081(31). \quad (3.3)$$

The result for L_{10}^r is the most precise to date, with, moreover, the errors purely data-driven. The result for $\mathcal{C}_1^r(\hat{\mu})$ lies significantly outside the range assumed in Ref. [6]. Its non-zero value also provides a further example of an LEC combination which vanishes in the large- N_c limit, but cannot be neglected for $N_c = 3$. The difference between our result for $\mathcal{C}_0^r(\hat{\mu})$ and that employed in Ref. [6], $0.00054(42)$, has two sources. The first is a shift in C_{61}^r due to significant shifts in the input to the analysis underlying the original C_{61}^r determination [14], the second the RChPT result for C_{80}^r used in Ref. [6], which turns out to represent a significant overestimate of the true value [18].

4. Acknowledgements

The lattice computations were done using the STFC's DiRAC facilities at Swansea and Edinburgh. PAB, LDD, NG and RJH are supported by an STFC Consolidated Grant, and by the EU under Grant Agreement PITN-GA-2009-238353 (ITN STRONGnet). EK was supported by the Comunidad Autónoma de Madrid under the program HEPHACOS S2009/ESP-1473 and the European Union under Grant Agreement PITN-GA-2009-238353 (ITN STRONGnet). KM acknowledges the hospitality of the CSSM, University of Adelaide and IFAE Barcelona, and the support of NSERC (Canada). JMZ is supported by the Australian Research Council grant FT100100005.

References

- [1] M. Davier, L. Girlanda, A. Höcker and J. Stern, *Phys. Rev.* **D58** (1998) 096014.
- [2] E. Shintani, *et al.*, *Phys. Rev. Lett.* **101** (2008) 202004.
- [3] P.A. Boyle, L. Del Debbio, J. Wennekens and J.M. Zanotti, *Phys. Rev.* **D81** 014504 (2010).
- [4] C. Aubin and T. Blum, *Phys. Rev.* **D75** (2006) 114502.
- [5] G. Amoros, J. Bijens and P. Talavera, *Nucl. Phys.* **B568** (2000) 319.
- [6] M. González-Alonso, A. Pich and J. Prades, *Phys. Rev.* **D78** (2008) 116012 (2008).
- [7] D. Boito *et al.*, *Phys. Rev.* **D87** (2013) 094008.
- [8] K. Ackerstaff, *et al.* (The OPAL Collaboration), *Eur. Phys. J.* **C7** (1999) 571.
- [9] D. Boito, *et al.*, *Phys. Rev.* **D84** (2011) 113006; *ibid.* **D85** (2012) 093015.
- [10] Y. Aoki *et al.*, *Phys. Rev.* **D83** (2011) 074508.
- [11] R. Arthur *et al.*, *Phys. Rev.* **D87** (2013) 094514.
- [12] J. Bijens, G. Colangelo and G. Ecker, *JHEP* **02** (1999) 020; *Ann. Phys.* **280** (2000) 100.
- [13] M. Jamin, J.A. Oller and A. Pich, *JHEP* **0402** (2004) 047.
- [14] S. Durr and J. Kambor, *Phys. Rev.* **D61** (2000) 114025.
- [15] K. Kampf and B. Moussallam, *Eur. Phys. J.* **C47** (2006) 723.
- [16] R. Unterdorfer and H. Pichl, *Eur. Phys. J.* **C55** (2008) 273.
- [17] J. Bijens and P. Talavera, *JHEP* **0203** (2002) 046.
- [18] K. Maltman, York University preprint YU-PP-I/E-KM-13-04.
- [19] J. Bijens and I. Jemos, *Nucl. Phys.* **B854** (2012) 631.
- [20] B. Aubert, *et al.* (The BaBar Collaboration), *Phys. Rev.* **D76** (2007) 051104; D. Epifanov, *et al.* (The Belle Collaboration), *Phys. Lett.* **B654** (2007) 65.
- [21] I.M. Nugent (for the BaBar Collaboration), arXiv:1301.7105 (hep-ex).
- [22] S. Ryu (for the Belle Collaboration), arXiv:1302.4565 (hep-ex).
- [23] R. Barate *et al.*, *Eur. Phys. J.* **C11** (1999) 599.